Reduced Elastodynamic Modelling of Parallel Robots for the Computation of their Natural Frequencies

S. Briot[*]
IRCCyN – CNRS
Nantes, France

A. Pashkevich[†]
IRCCyN – CNRS / Ecole des Mines de Nantes
Nantes, France

D. Chablat[‡]
IRCCyN – CNRS Nantes
Nantes, France

Abstract— *In this paper is presented an approach for computing the first natural frequencies of parallel robots. This approach, based on the Rayleigh-Ritz approximation, aims at reducing the model dimension by decreasing the size of the matrices describing the robot mass and stiffness, saving computational time and avoiding inaccuracy due to ill-conditioning. Thus it can be used in the design procedure as well as in real-time control. Simulations are carried out on a PRRRP robot modelled in 3D and comparisons with FEA software are presented.*

Keywords: elastodynamic modelling, model dimension reduction, natural frequencies, parallel robots.

I Introduction

Parallel robots have increasingly been used in industry in the last few years, mainly for pick-and-place applications or high-speed machining [1], [2]. This interest is due to their main properties, i.e. their higher rigidity and dynamic capacities compared with their serial manipulator counterparts.

Having a good knowledge of the elastodynamic behaviour of a manipulator (especially its natural frequencies) is a crucial point. In this sense, accurate elastodynamic models are necessary at both the control stage [3]–[5] and design stage [6]–[8], in order to optimize the geometry, as well as the shape of the elements of the manipulator. This will lead to the creation of a mechanism in which vibrations will be minimized.

Several models have been proposed and used in the literature in order to compute the natural frequencies of a mechanism during a preliminary design. Three main general methods can be distinguished:

- Finite element analysis (FEA); the FEA method is proved to be the most accurate and reliable, since the links/joints are modeled with its true dimension and shape [7], [9]–[12]. Its accuracy is limited by the discretization step only. However, because of high computational expenses required for the repeated re-meshing, this method is usually applied at the final design stage for the verification and component dimensioning.

- Matrix structural analysis (MSA) method is a common technique in mechanical engineering [13], [14]; it incorporates the main ideas of the FEA but operates with rather large flexible elements (beams, arcs, cables, etc.). This obviously yields reduction of the computational expense and, in some cases, allows analytical stiffness matrix to be obtained. However, this method can only be applied to links with simple shapes and requires improved skills in FEA.

- Virtual joint methods (VJM) [8], [15], which is also referred to as ''lumped modelling'', is based on the expansion of the traditional rigid model by adding virtual joints (localized springs), which describe the elastic deformations of the manipulator components (links, joints and actuators). Such kind of modelling is well adapted for links with complex shapes [16]. Generally, lumped modelling is simpler to use than MSA and provides acceptable accuracy in reduced computational time. It is widely used at the pre-design stage, especially for the analytical parametric analysis. However, due to the large number of virtual joints that have to be modelled in order to obtain good accuracy, such an approach is time-consuming. Moreover, for closed-loop mechanisms with passive joints, the way to assemble the matrices and to model the passive joints in kinematic chains is not straightforward.

The purpose of this paper is to propose a reduced elastodynamic modelling approach on parallel robots for the computation of the natural frequencies only, based on VJM. By keeping the simplicity of use of the VJM, this modelling considerably decreases the dimension of the problem by inverting only 6×6 matrices. It also proposes a straightforward procedure for the modelling of passive joints on parallel robots and for the assembly of the mass and stiffness matrices of closed-loop structures.

This paper will be organised as follows. Section 2 presents the theoretical background necessary in order to reduce the size of the elastodynamic model for the computation of the natural frequencies. In section 3, a numerical example is proposed in order to show the efficiency of our method. Finally, conclusions are drawn in section 4.

[*] Sebastien.Briot@irccyn.ec-nantes.fr
[†] Anatol.Pashkevich@emn.fr
[‡] Damien.Chablat@irccyn.ec-nantes.fr
[1] 13th World Congress in Mechanism and Machine Science, Guanajuato, México, 19-25 June, 2011

II. Theoretical background

A. Problem statement

Let us consider a general parallel manipulator made of n legs, each leg being composed of m links, m passive and one active joints, considered as ideal, i.e. without friction (Fig. 1a). Using the basic idea of VJM [15], let us decompose the j-th link of the i-th leg (denoted as the link ij where $j = 1, 2, …, m$ and $i = 1, 2, …, n$) into p_{ij} rigid elements and virtual springs (Fig. 1b). The mass and inertia matrix of the k-th rigid element of link ij (denoted as the element ijk) expressed in the local frame attached to this element, are denoted as m_{ijk} and $\mathbf{I}_{ijk}$, respectively. The displacement of its centre of mass S_{ijk} expressed in the base frame, resulting from the robot deformations, is denoted as $^{0}\mathbf{q}_{ijk} = [\,^{0}q_{ijk_1}, \,^{0}q_{ijk_2}, ..., \,^{0}q_{ijk_6}]^{T}$, where the first three components of this vector correspond to the translational displacements along the x, y and z axes of the base frame, respectively, and the last three components to the rotational displacements along the same axes. It should be mentioned that in the remainder of the paper, the left superscript "0" will stand for the coordinates expressed in the global frame. If no left superscript is mentioned, the vector is expressed in the local frame attached to the link ij.

The deformations of the k-th spring of link ij (denoted as the spring ijk) are denoted as $\boldsymbol{\theta}_{ijk} = [\theta_{ijk_1}, \theta_{ijk_2}, ..., \theta_{ijk_6}]^{T}$, where the three first components of this vector correspond to the translational deformations along the x, y and z axes of the base frame, respectively, and the last three components to the rotational deformations along the same axes. The kinetic energy of the system is equal to:

$$T = \frac{1}{2}\sum_{i=1}^{n}\sum_{j=1}^{m}\sum_{k=1}^{p_{ij}} {}^{0}\dot{\mathbf{q}}_{ijk}^{T} \, {}^{0}\mathbf{M}_{ijk} \, {}^{0}\dot{\mathbf{q}}_{ijk} = \frac{1}{2}\dot{\mathbf{q}}^{T}\mathbf{M}_{tot}\dot{\mathbf{q}} \quad (1)$$

where ${}^{0}\mathbf{M}_{ijk} = \mathrm{diag}(m_{ijk}\mathbf{I_3}, {}^{0}\mathbf{I}_{ijk})$, $\mathbf{I_3}$ being the identity matrix of dimension 3, $\dot{\mathbf{q}} = [{}^{0}\dot{\mathbf{q}}_{111}^{T}, {}^{0}\dot{\mathbf{q}}_{112}^{T}, ..., {}^{0}\dot{\mathbf{q}}_{nmp_{nm}}^{T}]^{T}$ is the vector regrouping all vectors ${}^{0}\dot{\mathbf{q}}_{ijk}$ (i.e. the velocity of the centre of masses S_{ijk}) and $\mathbf{M}_{tot}$ is the global mass matrix of the system.

The potential (elastic) energy of the system is equal to:

$$V_e = \frac{1}{2}\sum_{i=1}^{n}\sum_{j=1}^{m}\sum_{k=1}^{p_{ij}} \boldsymbol{\theta}_{ijk}^{T}\mathbf{K}_{ijk}\boldsymbol{\theta}_{ijk} \quad (2)$$
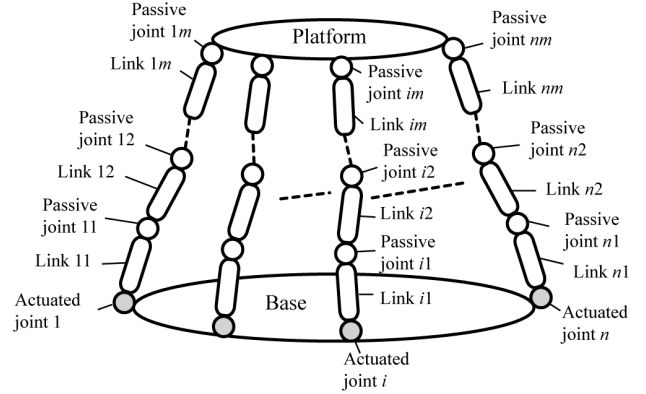
where $\mathbf{K}_{ijk}$ is the stiffness matrix of the virtual spring ijk.

It is shown in [8], [15] that the deformations $\boldsymbol{\theta}_{ijk}$ can be related to the displacements of the centres of masses of elements ijk and $ij(k+1)$ by the relation:
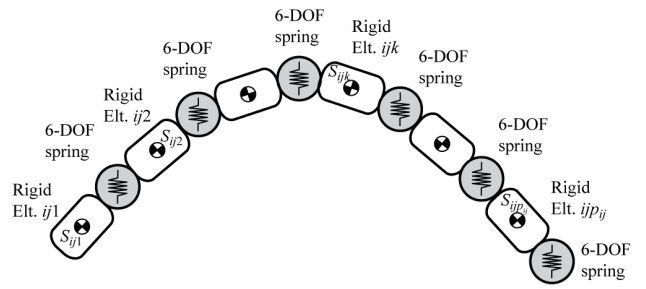
$$\boldsymbol{\theta}_{ijk} = \begin{bmatrix} \mathbf{C}_{2,ijk} & \mathbf{C}_{1,ij(k+1)} \end{bmatrix} \begin{bmatrix} {}^{0}\mathbf{q}_{ijk} \\ {}^{0}\mathbf{q}_{ij(k+1)} \end{bmatrix} \quad (3)$$

where $\mathbf{C}_{2,ijk}$ and $\mathbf{C}_{1,ij(k+1)}$ are two 6 by 6 matrices. Therefore, (2) can be rewritten as:

$$V_e = \frac{1}{2}\sum_{i,j,k} \begin{bmatrix} {}^{0}\mathbf{q}_{ijk}^{T} \\ {}^{0}\mathbf{q}_{ij(k+1)}^{T} \end{bmatrix} \begin{bmatrix} \mathbf{C}_{2,k}^{T} \\ \mathbf{C}_{1,k+1}^{T} \end{bmatrix} \mathbf{K}_{ijk} \begin{bmatrix} \mathbf{C}_{2,k}^{T} \\ \mathbf{C}_{1,k+1}^{T} \end{bmatrix}^{T} \begin{bmatrix} {}^{0}\mathbf{q}_{ijk} \\ {}^{0}\mathbf{q}_{ij(k+1)} \end{bmatrix} = \frac{1}{2}\mathbf{q}^{T}\mathbf{K}_{tot}\mathbf{q} \quad (4)$$

(a) Architectural representation

(b) Elastic representation of one link

Fig. 1. A general parallel manipulator.

where $\mathbf{q} = [{}^{0}\mathbf{q}_{111}^{T}, {}^{0}\mathbf{q}_{112}^{T}, ..., {}^{0}\mathbf{q}_{nmp_{nm}}^{T}]^{T}$ is the vector regrouping all vectors ${}^{0}\mathbf{q}_{ijk}$ and $\mathbf{K}_{tot}$ is the global stiffness matrix of the system.

Starting from these definitions, and considering that the robot is in an equilibrium position and no external forces are applied, the authors of [15] demonstrate that the system is governed by the relation:

$$\mathbf{M}_{tot}\ddot{\mathbf{q}} + \mathbf{K}_{tot}\mathbf{q} = \mathbf{0} . \quad (5)$$

A solution $\mathbf{q}_l$ of this equation can be found by solving the system:

$$\left(\omega_l^2\mathbf{M}_{tot} - \mathbf{K}_{tot}\right)\mathbf{q}_l = \mathbf{0} , \text{ with } \omega_l = 2\pi f_l \quad (6)$$

where $\mathbf{q}_l$ represents the vectors of the shape of free vibrations of the system for the l-th natural mode, f_l and ω_l are their corresponding natural frequency and pulsation, respectively.

If the matrix $\omega_l^2\mathbf{M}_{tot} - \mathbf{K}_{tot}$ is singular (which is always the case when ω_l is one of the modal pulsation of the robot), $\mathbf{q}_l$ becomes non-null and is the eigenvector corresponding to the pulsation ω_l. There is an infinity of vectors $\mathbf{q}_l$ validating (6) (for a given ω_l), but all are proportional to the others. Vector $\mathbf{q}_l$ is not necessarily dependent of time, but almost represents the amplitude of the vibrations. Therefore, when *only* the l-th mode of the system is excited, the displacements of all springs may be written under the form:

$$\mathbf{q}_l^{*} = \mathbf{q}_l \sin(\omega_l t + \varphi_l) \quad (7)$$

2

where φ_l is a phase difference corresponding to the mode l. When all modes are excited, the displacement $\mathbf{q}$ of all spring centres may be written in the form:

$$\mathbf{q} = \sum_{l=1}^{6d} \mathbf{q}_l^* = \sum_{l=1}^{6d} \mathbf{q}_l \sin(\omega_l t + \varphi_l) \qquad (8)$$

The most common way to find the values of the pulsation ω_l is to solve the eigenvalue problem

$$\det\left(\omega_l^2 \mathbf{I} - \mathbf{M}_{tot}^{-1} \mathbf{K}_{tot} \right) = 0 . \qquad (9)$$

where $\mathbf{I}$ is an identity matrix of dimension 6 d, with $d = n\,m\sum_{i,j} p_{ij}$.

However, solving this problem involves finding the 6 d eigenvalues of the problem and also inverting the d matrices $\mathbf{M}_{ijk}$ constituting the matrix $\mathbf{M}_{tot}$, which is highly time-consuming and can lead to few accurate results because of the problem dimension.

In order to avoid such kind of drawbacks [16] has recently proposed (for elastostatic modelling only) a new procedure to compute the deformations of the robot when a force is applied at the end-effector. This procedure computes a stiffness (and also compliance) matrix $\mathbf{K_r}$ (and $\mathbf{S_r}$, resp.) of dimension 6 that represents the behaviour of the robot in terms of deformations. Moreover, during the procedure, only inversions of 6 dimensional matrices are involved, which considerably reduces computational time and avoids accuracy problems due to ill-conditioning of the large global stiffness matrix. Thus, the global 6 d dimensional problem defined with respect to all variables $\mathbf{q}$ has been reduced to a 6 dimensional problem defined with respect to platform deflections $\delta\mathbf{t}$ only. As a result, the entire robot can locally be seen as a virtual spring of dimension 6 that deforms when applying a wrench on the end-effector.

Starting from these considerations, it would be interesting to reduce the dimension of the problem by expressing Eq. (6) as a function of the reduced stiffness matrix $\mathbf{K_r}$, of the platform deflections $\delta\mathbf{t}$ and, also, as a function of a reduced mass matrix that will be denoted as $\mathbf{M_r}$, which could represent the global behaviour of the robot in terms of natural frequencies. The remainder of the paper will focus on this problem.

B. Rayleigh-Ritz approximation

Another way to find the natural pulsation ω_l of the mode l would be to know the exact amplitude $\boldsymbol{\Phi}_l$ of the displacements $\mathbf{q}_l$ for this mode. For the natural mode l, the potential and kinetic energies of the system are given by:

$$V_e = \frac{1}{2}\mathbf{q}_l^{*T}\mathbf{K}_{tot}\mathbf{q}_l^* = \frac{1}{2}\mathbf{q}_l^T\mathbf{K}_{tot}\mathbf{q}_l \sin^2\left(\omega_l t + \varphi_l\right) \qquad (10a)$$

$$T = \frac{1}{2}\dot{\mathbf{q}}_l^{*T}\mathbf{M}_{tot}\dot{\mathbf{q}}_l^* = \frac{1}{2}\omega_l^2\mathbf{q}_l^T\mathbf{M}_{tot}\mathbf{q}_l \cos^2\left(\omega_l t + \varphi_l\right) \qquad (10b)$$

From the principle of energy conservation, it follows that

$$\max\left(V_e\right) - \max\left(T\right) = 0 , \text{ i.e } \mathbf{q}_l^T\left(\omega_l^2\mathbf{M}_{tot} - \mathbf{K}_{tot}\right)\mathbf{q}_l = 0 \quad (11)$$

which is an univariate equation in ω_l.

It is obvious that the exact knowledge of the amplitude $\mathbf{q}_l$ is an impossible task without a direct measure on the system of all the displacements of the robot nodes. However, this vector may be approximated by another denoted as $\hat{\mathbf{q}}_l$ that is close to the exact amplitude $\mathbf{q}_l$. Introducing this approximated vector $\hat{\mathbf{q}}_l$ into (10) will allow us to find a corresponding value of $\hat{\omega}_l$ and, as a result, $\hat{f}_l$ which is the approximated natural frequency of the system. Such kind of elastodynamic problem resolution is called the Rayleigh-Ritz method [17].

The better the approximation, the more accurate the value of $\hat{\omega}_l$. The designer's skills in terms of understanding and analysis of robot physical behaviour here are of the utmost importance. In this sense, let us recall that the first natural frequencies are associated with the highest level of energy due to vibrations, and represent the highest displacements of the structure. Therefore, in design optimization loops, it is essential to maximize the value of the first frequency.

Using the Rayleigh-Ritz approximation in order to compute the first natural frequencies, the stresses for which the maximal displacements appear have to be found. From our experience in elastic behaviour of robots, it is assumed that a good approximation of these maximal displacements will be the deformation of the robot with a load applied at the end-effector, and it can be shown in the following that this hypothesis is valid. Using this assumption, the displacements $\mathbf{q}_l$ of all springs can be computed as a function of the end-effector displacements $\delta\mathbf{t}$, i.e. it is possible to define a matrix $\mathbf{J_q}$ such as:

$$\mathbf{q}_l = \mathbf{J_q}\delta\mathbf{t} . \qquad (12)$$

As a result, introducing (12) into (11) will lead to

$$\delta\mathbf{t}^T\left(\omega_l^2\mathbf{J_q}^T\mathbf{M}_{tot}\mathbf{J_q} - \mathbf{J_q}^T\mathbf{K}_{tot}\mathbf{J_q}\right)\delta\mathbf{t} = \mathbf{0} \qquad (13)$$

where the matrices $\mathbf{J_q}^T\mathbf{M}_{tot}\mathbf{J_q}$ and $\mathbf{J_q}^T\mathbf{K}_{tot}\mathbf{J_q}$ are now of dimension 6. It should be mentioned here that, in the case where an external load is applied at the end-effector only, the term $\mathbf{J_q}^T\mathbf{K}_{tot}\mathbf{J_q}$ is equal to the reduced stiffness matrix $\mathbf{K_r}$ of the robot. Therefore, (13) can be rewritten as:

$$\delta\mathbf{t}^T\left(\omega_l^2\mathbf{M_r} - \mathbf{K_r}\right)\delta\mathbf{t} = \mathbf{0} , \text{ with } \mathbf{M_r} = \mathbf{J_q}^T\mathbf{M}_{tot}\mathbf{J_q} \qquad (14)$$

In the following sections it is explained how to obtain expressions (12) and (14).

C. Reduction of the link mass matrix

It is possible to decompose the previously cited task into two sub-problems. First, the displacements of each spring in the beam ij can be expressed as a function of the displacement of its extremities. Then, one can express the

beam extremity displacements as a function of the platform displacements δ**t**. Using this approach will allow for a reduction in the size of the link mass matrices, and thus avoiding creating global mass matrices $\mathbf{M}_{tot}$ with very large dimension.

Two main ways can be followed to reduce the size of the link mass matrices. The first one consists in discretizing the link ij into p_{ij} rigid links and springs and to express their displacements as a function of the beam extremity displacements. However, such numerical method must be repeated for each link and, thus, increases the size of the algorithm and decreases its efficiency. As a result, it is prefered to use the following procedure which allows analytical expressions to be obtained for the reduced link mass matrices.

Let us consider the link ij, modelled as a beam (Fig. 2). At this beam is attached a local frame represented by the vectors $\mathbf{x_{ij}}$, $\mathbf{y_{ij}}$ and $\mathbf{z_{ij}}$. Before any deformation of the system, the beam ij is linked (rigidly or by a passive joint) to beams $i(j–1)$ and $i(j+1)$ at points O_{ij} and $O_{i(j+1)}$, respectively (Fig. 2). After deformation of the robot, the beam extremity located at O_{ij} is displaced from $\mathbf{q_{ij}^1} = [q_{ij_1}^1, q_{ij_2}^1, ..., q_{ij_6}^1]^T$ and the one located at $O_{i(j+1)}$ is displaced from $\mathbf{q_{ij}^2} = [q_{ij_1}^2, q_{ij_2}^2, ..., q_{ij_6}^2]^T$, where the three first components of each vector correspond to the translational displacements along local $\mathbf{x_{ij}}$, $\mathbf{y_{ij}}$ and $\mathbf{z_{ij}}$ axes, respectively, and the three last components to the rotational displacements along the same axes.

The general formula for the kinetic energy of an elastic Bernoulli beam is equal to [14]:

$$T_{ij} = \frac{1}{2} \int_0^{L_{ij}} \rho_{ij} \dot{\mathbf{q}}_{\mathbf{ij}}^T \mathbf{Q_{ij}} \dot{\mathbf{q}}_{\mathbf{ij}} dx \qquad (15)$$

with $\mathbf{Q_{ij}} = \mathrm{diag}(A_{ij}, A_{ij}, A_{ij}, I_{ij}^p, I_{ij}^y, I_{ij}^z)$. In this expression, $\dot{\mathbf{q}}_{\mathbf{ij}}$ represents the velocity of the beam cross-section located at position x from the local reference frame (Fig. 2), L_{ij} is the length of the beam ij, ρ_{ij} the mass density at cross-section x, A_{ij} its area, I_{ij}^p its torsional constant and I_{ij}^y, I_{ij}^z the quadratic momentums along $\mathbf{y_{ij}}$ and $\mathbf{z_{ij}}$, respectively.

For the l-th natural mode, and from (7), the kinetic energy can be rewritten as:

$$T_{ij} = \frac{1}{2} \omega_l^2 \cos^2 \left(\omega_l t + \varphi_l \right) \int_0^{L_{ij}} \rho_{ij} \mathbf{q}_{\mathbf{ij}}^T \mathbf{Q_{ij}} \mathbf{q}_{\mathbf{ij}} dx \qquad (16)$$

$\mathbf{q_{ij}}$ being the amplitude of the displacement of the beam cross-section located at position x from the local reference frame (Fig. 2).

In the Rayleigh-Ritz approximation, considering that the deformations due to the natural vibrations are similar to those obtained when an external load is applied at the robot end-effector only, each link of the structure will deform due to the stresses transmitted through the robot joints at points O_{ij}. As a result, the deformations $\boldsymbol{\delta_{ij}}$
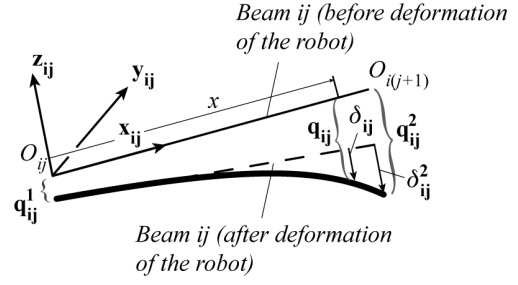

Fig. 2. Displacements and elastic deformations of a beam.

of the beam cross-section (Fig. 2) can be approximated by the deformations of a tip-loaded beam, given by [14]:

$$\boldsymbol{\delta_{ij}} = \mathrm{diag}(f_{ij}, g_{ij}, g_{ij}, f_{ij}, h_{ij}, h_{ij}) \boldsymbol{\delta_{ij}^2} \qquad (17)$$

where $\boldsymbol{\delta_{ij}^2} = \boldsymbol{\delta_{ij}}(x = L_{ij})$ represents the deformation of the beam at its tip and

$$f_{ij}(x) = x / L_{ij} , \qquad (18a)$$

$$g_{ij}(x) = 0.5x^2 (3L_{ij} - x) / L_{ij}^3 , \qquad (18b)$$

$$h_{ij}(x) = x(L_{ij} - 0.5x) / L_{ij}^2 . \qquad (18c)$$

As a result, the global displacement $\mathbf{q_{ij}}$ of the beam cross-section at x can be expressed as a sum of two terms:

$$\mathbf{q_{ij}} = \begin{bmatrix} \mathbf{I}_3 & \mathbf{D}_{(x)} \\ \mathbf{0}_3 & \mathbf{I}_3 \end{bmatrix} \mathbf{q_{ij}^1} + \boldsymbol{\delta_{ij}} \text{ where } \mathbf{D}_{(x)} = \begin{bmatrix} 0 & 0 & 0 \\ 0 & 0 & -x \\ 0 & x & 0 \end{bmatrix} \quad (19)$$

In this sum, the left terms corresponds to the displacement of the undeformed beam due to the displacement of the node located at O_{ij}.

In the hypothesis that the beam cross-section is constant, introducing (17) and (19) into (16), and integrating, leads to:

$$T_{ij} = \frac{1}{2} \omega_l^2 \cos^2 \left(\omega_l t + \varphi_l \right) \left(\left[(\mathbf{q_{ij}^1})^T \ (\boldsymbol{\delta_{ij}^2})^T \right] \mathbf{M_{ij}} \begin{bmatrix} \mathbf{q_{ij}^1} \\ \boldsymbol{\delta_{ij}^2} \end{bmatrix} \right) \quad (20)$$

where $\mathbf{M_{ij}} = \begin{bmatrix} \mathbf{M_{ij}^{11}} & \mathbf{M_{ij}^{12}} \\ (\mathbf{M_{ij}^{12}})^T & \mathbf{M_{ij}^{22}} \end{bmatrix}$ with

$$\mathbf{M_{ij}^{11}} = \begin{bmatrix} m_{ij} & 0 & 0 & 0 & 0 & 0 \\ 0 & m_{ij} & 0 & 0 & 0 & m_{ij}L_{ij}/2 \\ 0 & 0 & m_{ij} & 0 & -m_{ij}L_{ij}/2 & 0 \\ 0 & 0 & 0 & {}^{ij}I_{ij}^p \rho_{ij}L_{ij} & 0 & 0 \\ 0 & 0 & -m_{ij}L_{ij}/2 & 0 & m_{ij}L_{ij}^2/3 + {}^{ij}I_{ij}^y \rho_{ij}L_{ij} & 0 \\ 0 & m_{ij}L_{ij}/2 & 0 & 0 & 0 & m_{ij}L_{ij}^2/3 + {}^{ij}I_{ij}^z \rho_{ij}L_{ij} \end{bmatrix} \quad (21a)$$

$$\mathbf{M_{ij}^{12}} = \begin{bmatrix} m_{ij}/2 & 0 & 0 & 0 & 0 & 0 \\ 0 & 3m_{ij}/8 & 0 & 0 & 0 & 0 \\ 0 & 0 & 3m_{ij}/8 & 0 & 0 & 0 \\ 0 & 0 & 0 & {}^{ij}I_{ij}^p \rho_{ij}L_{ij}/2 & 0 & 0 \\ 0 & 0 & -11m_{ij}L_{ij}/40 & 0 & 2^{ij}I_{ij}^y \rho_{ij}L_{ij}/3 & 0 \\ 0 & 11m_{ij}L_{ij}/40 & 0 & 0 & 0 & 2^{ij}I_{ij}^z \rho_{ij}L_{ij}/3 \end{bmatrix} \quad (21b)$$

$$\mathbf{M_{ij}^{22}} = \mathrm{diag}\left(\frac{m_{ij}}{3}, \frac{33m_{ij}}{140}, \frac{33m_{ij}}{140}, \frac{I_{ij}^p \rho_{ij}L_{ij}}{3}, \frac{8}{15}I_{ij}^y \rho_{ij}L_{ij}, \frac{8}{15}I_{ij}^z \rho_{ij}L_{ij} \right) \quad (21c)$$

It should be mentioned that, in the case where the section of the beam is not constant, (18) to (21) are no more correct. In this case, the deformation of the beam and its kinetic energy should be obtained numerically.

From (17), it can be shown that:

$$\boldsymbol{\delta}_{ij}^2 = \mathbf{q}_{ij}^2 - \begin{bmatrix} \mathbf{I}_3 & \mathbf{D}_{(L_{ij})} \\ \mathbf{0}_3 & \mathbf{I}_3 \end{bmatrix} \mathbf{q}_{ij}^1 . \tag{22}$$

which leads to:

$$\begin{bmatrix} \mathbf{q}_{ij}^1 \\ \boldsymbol{\delta}_{ij}^2 \end{bmatrix} = \begin{bmatrix} \mathbf{I}_6 & \mathbf{0}_6 \\ \mathbf{E}_{ij}^{21} & \mathbf{I}_6 \end{bmatrix} \begin{bmatrix} \mathbf{q}_{ij}^1 \\ \mathbf{q}_{ij}^2 \end{bmatrix} = \mathbf{E}_{ij} \begin{bmatrix} \mathbf{q}_{ij}^1 \\ \mathbf{q}_{ij}^2 \end{bmatrix}, \ \mathbf{E}_{ij}^{21} = -\begin{bmatrix} \mathbf{I}_3 & \mathbf{D}_{(L_{ij})} \\ \mathbf{0}_3 & \mathbf{I}_3 \end{bmatrix} \tag{23}$$

Introducing (23) into (20) leads to:

$$T_{ij} = \frac{1}{2} \omega_l^2 \cos^2\left(\omega_l t + \varphi_l\right)\left(\begin{bmatrix} \mathbf{q}_{ij}^1 \\ \mathbf{q}_{ij}^2 \end{bmatrix}^T \mathbf{E}_{ij}^T \mathbf{M}_{ij} \mathbf{E}_{ij} \begin{bmatrix} \mathbf{q}_{ij}^1 \\ \mathbf{q}_{ij}^2 \end{bmatrix}\right) \tag{24}$$

Expressing vectors $\mathbf{q}_{ij}^v$ ($v = 1, 2$) in the base frame, (24) becomes:

$$T_{ij} = \frac{1}{2} \omega_l^2 \cos^2\left(\omega_l t + \varphi_l\right)\left(\begin{bmatrix} {}^0\mathbf{q}_{ij}^1 \\ {}^0\mathbf{q}_{ij}^2 \end{bmatrix}^T {}^0\mathbf{M}_{ij}^{red} \begin{bmatrix} {}^0\mathbf{q}_{ij}^1 \\ {}^0\mathbf{q}_{ij}^2 \end{bmatrix}\right) \tag{25}$$

where $\ {}^0\mathbf{M}_{ij}^{red} = \mathbf{R}_{0ij} \left(\mathbf{E}_{ij}\right)^T \mathbf{M}_{ij} \mathbf{E}_{ij} \mathbf{R}_{0ij}^T \ $ and $\mathbf{R}_{0ij}$ is the rotation matrix from the local frame of beam ij to the global frame, i.e.

$$\begin{bmatrix} {}^0\mathbf{q}_{ij}^1 \\ {}^0\mathbf{q}_{ij}^2 \end{bmatrix} = \mathbf{R}_{0ij} \begin{bmatrix} \mathbf{q}_{ij}^1 \\ \mathbf{q}_{ij}^2 \end{bmatrix} . \tag{26}$$

To show the validity of the approach, let us compare the obtained equations when they are applied on a single beam fixed at one extremity O_{11}, i.e. $\ {}^0\mathbf{q}_{11}^1 = \mathbf{0}$. For the numerical example, it is considered that this beam has the following characteristics:
- length $L = 1$ m
- hollow circular cross-section of external diameter 40 mm and internal diameter 30 mm
- material: steel (Young modulus $E = 204$ GPa, Poisson coefficient $v = 0.3$, density $\rho = 8020$ kg/m^3)

For such an element, beam theory gives the following expressions for the natural frequencies [17]:
- 1st natural frequency due to transverse displacements:

$$f_{tr} = \frac{3.516}{2\pi L^2} \sqrt{\frac{EI^z}{m}} = 35.28 \, \text{Hz} \tag{27a}$$

where m is the mass of the beam and I^z its quadratic momentum along $\mathbf{z}$ axis.
- 1st natural frequency due to longitudinal displacements:

$$f_l = \sqrt{E/\rho}\big/(4L) = 1260.86 \, \text{Hz} \tag{27b}$$

- 1st natural frequency due to torsional displacements:

$$f_{to} = \sqrt{I^p G/(I^y + I^z)}\big/(4L) = 781.95 \, \text{Hz} \tag{27c}$$

where G is the shear modulus, I^y its quadratic momentum along $\mathbf{y}$ axis and I^p its torsional constant.

Applying the previously developed equations to this case by considering that the reduced mass matrix $\mathbf{M_r} = \mathbf{M}_{11}^{22}$ is given at (21c) and the stiffness matrix $\mathbf{K_r}$ is expressed in [16] as:

$$\mathbf{K_r} = \frac{1}{L} \begin{bmatrix} ES & 0 & 0 & 0 & 0 & 0 \\ 0 & 12EI^z/L^2 & 0 & 0 & 0 & -6EI^z/L \\ 0 & 0 & 12EI^y/L^2 & 0 & 6EI^y/L & 0 \\ 0 & 0 & 0 & GI^p & 0 & 0 \\ 0 & 0 & 6EI^y/L & 0 & 4EI^y & 0 \\ 0 & -6EI^z/L & 0 & 0 & 0 & 4EI^z \end{bmatrix}, \tag{28}$$

it is found:
- 1st natural frequency due to transversal displacements: 35.78 Hz (error of 1.4%)
- 1st natural frequency due to longitudinal displacements: 1390.30 Hz (error of 10.27%)
- 1st natural frequency due to torsional displacements: 862.23 Hz (error of 10.27%)

As a conclusion, the proposed reduced model is accurate enough for the computation of the first natural frequency due to transversal displacements, which is also the first natural frequency of the beam.

Let us now reduce the size of the total mass matrix of the robot.

D. Reduction of the robot mass matrix

Using the results of the previous section, the total kinetic energy of the system is given by:

$$T = \sum_{i,j} T_{ij} = \frac{1}{2} \omega_l^2 \cos^2\left(\omega_l t + \varphi_l\right) \sum_{i,j} \left(\begin{bmatrix} {}^0\mathbf{q}_{ij}^1 \\ {}^0\mathbf{q}_{ij}^2 \end{bmatrix}^T {}^0\mathbf{M}_{ij}^{red} \begin{bmatrix} {}^0\mathbf{q}_{ij}^1 \\ {}^0\mathbf{q}_{ij}^2 \end{bmatrix}\right) \tag{29}$$

$$= \frac{1}{2} \omega_l^2 \cos^2\left(\omega_l t + \varphi_l\right) \mathbf{q}^T \mathbf{M}_{tot} \mathbf{q}$$

with $\mathbf{M}_{tot} = diag({}^0\mathbf{M}_{11}^{red}, {}^0\mathbf{M}_{12}^{red}, ..., {}^0\mathbf{M}_{nm}^{red})$ and

$$\mathbf{q}^T = \left[\left({}^0\mathbf{q}_{11}^1\right)^T, \left({}^0\mathbf{q}_{11}^2\right)^T, \left({}^0\mathbf{q}_{12}^1\right)^T, \left({}^0\mathbf{q}_{12}^2\right)^T, ..., \left({}^0\mathbf{q}_{nm}^1\right)^T, \left({}^0\mathbf{q}_{nm}^2\right)^T\right].$$

It is necessary to express the relationship linking all vectors $\ {}^0\mathbf{q}_{ij}^v$ ($v = 1, 2$) to the end-effector displacements $\boldsymbol{\delta}\mathbf{t}$. From [16], this displacement is equal to:

$$\boldsymbol{\delta}\mathbf{t} = \mathbf{J}_{\theta i}\boldsymbol{\theta}_i + \mathbf{J}_{pi}\mathbf{p}_i , \tag{30}$$

where $\boldsymbol{\theta}_i$ represents the deformations of all virtual springs of the leg i and $\mathbf{p}_i$ the displacements of its passive joints, and $\mathbf{J}_{\theta i}$ and $\mathbf{J}_{pi}$ are Jacobian matrices relying these displacements to the displacement $\boldsymbol{\delta}\mathbf{t}$. These matrices can be obtained by the differentiation of the global transformation matrix $\mathbf{T}^i$ of the chain i including rigid, passive and elastic coordinates [16]. The way to obtain these matrices is explained in more depth in the next section. It should be mentioned that the dimension of $\mathbf{J}_{pi}$ is 6 by m, m being the number of passive joints of the leg, with $m < 6$ (because one leg of a parallel robot cannot have more than five passive degrees of freedom (DOF)).

From [16], it can also be shown that:

$$\boldsymbol{\delta}\mathbf{t} = \mathbf{J}_{\theta i}\mathbf{S}_{\theta i}\mathbf{J}_{\theta i}^T\mathbf{f}_i + \mathbf{J}_{pi}\mathbf{p}_i , \tag{31}$$

where $\mathbf{S}_{\boldsymbol{\theta}i}$ is a block-diagonal matrix regrouping all the compliance matrices of each virtual springs, and $\mathbf{f}_i$ is the force applied on the i that involves the displacement $\delta\mathbf{t}$. The expression of $\mathbf{f}_i$ is such as

$$\mathbf{f}_i = \mathbf{K}_i \delta\mathbf{t} \qquad (32)$$

$\mathbf{K}_i$ being the global stiffness matrix of the leg i. Introducing (32) into (31) leads to:

$$\left(\mathbf{I} - \mathbf{J}_{\boldsymbol{\theta}i}\mathbf{S}_{\boldsymbol{\theta}i}\mathbf{J}_{\boldsymbol{\theta}i}^T\mathbf{K}_i\right)\delta\mathbf{t} = \mathbf{J}_{\mathbf{p}i}\,\mathbf{p}_i . \qquad (33)$$

Therefore, the displacements $\mathbf{p}_i$ of the robot passive joints due to the displacement $\delta\mathbf{t}$ are equal to:

$$\mathbf{p}_i = \left(\mathbf{J}_{\mathbf{p}i}^T\mathbf{J}_{\mathbf{p}i}\right)^{-1}\mathbf{J}_{\mathbf{p}i}^T\left(\mathbf{I} - \mathbf{J}_{\boldsymbol{\theta}i}\mathbf{S}_{\boldsymbol{\theta}i}\mathbf{J}_{\boldsymbol{\theta}i}^T\mathbf{K}_i\right)\delta\mathbf{t} = \mathbf{J}_{\mathbf{tp}i}\,\delta\mathbf{t} . \qquad (34)$$

Let us now compute the displacements $^0\mathbf{q}_{\mathbf{ij}}^2$ of the virtual spring located at the extremity of the link ij. This spring ij is preceded by j–1 other virtual springs and passive joints. The deformations of the j springs (including the one at the link extremity) will be denoted as $\boldsymbol{\theta}_{ij}$, and the displacements of the j–1 passive joints $\mathbf{p}_{ij}$, respectively. They can be related to the displacement $^0\mathbf{q}_{\mathbf{ij}}^2$ by the Jacobian matrices $\mathbf{J}_{\boldsymbol{\theta}ij}$ and $\mathbf{J}_{\mathbf{p}ij}$ as

$$^0\mathbf{q}_{\mathbf{ij}}^2 = \mathbf{J}_{\boldsymbol{\theta}ij}\,\boldsymbol{\theta}_{ij} + \mathbf{J}_{\mathbf{p}ij}\,\mathbf{p}_{ij} , \qquad (35)$$

These matrices may be computed in a similar way to the matrices $\mathbf{J}_{\boldsymbol{\theta}i}$ and $\mathbf{J}_{\mathbf{p}i}$, but by considering the truncated chain i going from the base to the virtual spring ij. The deformations $\boldsymbol{\theta}_{ij}$ involve constraints into the j virtual springs of the truncated chain that are denoted as $\boldsymbol{\tau}_{ij}$. Their expressions may be found from the relationship [16]:

$$\mathbf{S}_{\boldsymbol{\theta}ij}\,\boldsymbol{\tau}_{ij} = \boldsymbol{\theta}_{ij} , \qquad (36)$$

where $\mathbf{S}_{\boldsymbol{\theta}ij}$ is a block-diagonal matrix regrouping all the compliance matrices of the j virtual springs of the truncated chain. Introducing (34) into (33) leads to:

$$^0\mathbf{q}_{\mathbf{ij}}^2 = \mathbf{J}_{\boldsymbol{\theta}ij}\mathbf{S}_{\boldsymbol{\theta}ij}\,\boldsymbol{\tau}_{ij} + \mathbf{J}_{\mathbf{p}ij}\mathbf{p}_{ij} . \qquad (37)$$

Let us consider now the entire leg i of the mechanism. The constraints $\boldsymbol{\tau}_i$ applied to the springs due to the force $\mathbf{f}_i$ applied on the platform are given by [16],

$$\boldsymbol{\tau}_i = \begin{bmatrix} \boldsymbol{\tau}_{ij} \\ \boldsymbol{\tau}_{ir} \end{bmatrix} = \mathbf{J}_{\boldsymbol{\theta}i}^T\mathbf{f}_i = \begin{bmatrix} \mathbf{J}_{j\boldsymbol{\theta}i}^T \\ \mathbf{J}_{\bar{j}\boldsymbol{\theta}i}^T \end{bmatrix}\mathbf{f}_i , \qquad (38)$$

where $\mathbf{J}_{j\boldsymbol{\theta}i}$ corresponds to the j first columns of matrix $\mathbf{J}_{\boldsymbol{\theta}i}$. Introducing (38) into (37),

$$^0\mathbf{q}_{\mathbf{ij}}^2 = \mathbf{J}_{\boldsymbol{\theta}ij}\mathbf{S}_{\boldsymbol{\theta}ij}\mathbf{J}_{j\boldsymbol{\theta}i}^T\mathbf{f}_i + \mathbf{J}_{\mathbf{p}ij}\mathbf{p}_{ij} = \mathbf{J}_{\boldsymbol{\theta}ij}\mathbf{S}_{\boldsymbol{\theta}ij}\mathbf{J}_{j\boldsymbol{\theta}i}^T\mathbf{K}_i\delta\mathbf{t} + \mathbf{J}_{\mathbf{p}ij}\mathbf{p}_{ij} . \qquad (39)$$

Moreover, the passive displacements $\mathbf{p}_{ij}$ are known from expression (32). Considering that $\mathbf{J}_{j\mathbf{tp}i}$ represents the matrix composed of the j first lines of $\mathbf{J}_{\mathbf{tp}i}$ given at (32), it follows that

$$^0\mathbf{q}_{\mathbf{ij}}^2 = \left(\mathbf{J}_{\boldsymbol{\theta}ij}\mathbf{S}_{\boldsymbol{\theta}ij}\mathbf{J}_{j\boldsymbol{\theta}i}^T\mathbf{K}_i + \mathbf{J}_{\mathbf{p}ij}\mathbf{J}_{j\mathbf{tp}ij}\right)\delta\mathbf{t} = \mathbf{J}_{\mathbf{ij}}^{\mathbf{q}_2}\delta\mathbf{t} . \qquad (40)$$

Once all $^0\mathbf{q}_{\mathbf{ij}}^2$ are found, the vectors $^0\mathbf{q}_{\mathbf{ij}}^1$ can be computed. Indeed, displacement $^0\mathbf{q}_{\mathbf{ij}}^1$ is nothing none than displacement $^0\mathbf{q}_{\mathbf{i(j-1)}}^1$ plus the small deflection of the passive joint located at O_{ij}, i.e.:

$$^0\mathbf{q}_{\mathbf{ij}}^1 = {}^0\mathbf{q}_{\mathbf{i(j-1)}}^2 + {}^0\mathbf{s}_{\mathbf{ij}}\,\delta p_{ij} \qquad (41)$$

where δp_{ij} is the value of the displacement of the passive joint located at O_{ij} and $^0\mathbf{s}_{\mathbf{ij}}$ is a unit screw corresponding to its twist. Introducing (34) and (40) into (41):

$$^0\mathbf{q}_{\mathbf{ij}}^1 = \mathbf{J}_{\mathbf{ij}}^{\mathbf{q}_2}\delta\mathbf{t} + {}^0\mathbf{s}_{\mathbf{ij}}\mathbf{J}_{j\mathbf{tp}i}^*\,\delta\mathbf{t} = \left(\mathbf{J}_{\mathbf{ij}}^{\mathbf{q}_2} + {}^0\mathbf{s}_{\mathbf{ij}}\mathbf{J}_{j\mathbf{tp}i}^*\right)\delta\mathbf{t} = \mathbf{J}_{\mathbf{ij}}^{\mathbf{q}_1}\delta\mathbf{t} \quad (42)$$

where $\mathbf{J}_{j\mathbf{tp}i}^*$ is the j-th line of matrix $\mathbf{J}_{\mathbf{tp}i}$ given at (32).

Thus, from (40) and (42), one can express vector $\mathbf{q}$ given at (29) as a function $\delta\mathbf{t}$ as follows:

$$\mathbf{q} = \left[\left(\mathbf{J}_{\mathbf{11}}^{\mathbf{q}_1}\right)^T, \left(\mathbf{J}_{\mathbf{11}}^{\mathbf{q}_2}\right)^T, \left(\mathbf{J}_{\mathbf{12}}^{\mathbf{q}_1}\right)^T, \left(\mathbf{J}_{\mathbf{12}}^{\mathbf{q}_2}\right)^T, ..., \left(\mathbf{J}_{\mathbf{nm}}^{\mathbf{q}_1}\right)^T, \left(\mathbf{J}_{\mathbf{nm}}^{\mathbf{q}_2}\right)^T\right]^T \delta\mathbf{t} \quad (43)$$
$$= \mathbf{J}_{\mathbf{q}}\delta\mathbf{t}$$

Introducing this relation into (29) will lead to:

$$T = \frac{1}{2}\omega_l^2\cos^2\left(\omega_l t + \varphi_l\right)\delta\mathbf{t}^T\mathbf{M}_{\mathbf{r}}\delta\mathbf{t} \qquad (44)$$

where the expression of $\mathbf{M}_{\mathbf{r}}$ is given at (14).

As a result, from (14), finding the robot natural frequencies relies on solving the 6 dimensional eigenvalues problem

$$\det\left(\omega_l^2\mathbf{I}_{\mathbf{6}} - \mathbf{M}_{\mathbf{r}}^{-1}\mathbf{K}_{\mathbf{r}}\right) = 0 . \qquad (45)$$

Let us now apply this method using an example.

III. Case study

In this section, the example of the planar _PRRRP_[2] manipulator with two parallel prismatic axes (Fig. 3) will be treated. Let us first compute the global 3D stiffness matrix $\mathbf{K}_{\mathbf{r}}$ of the robot.

The method presented in [16] states that each leg may be decomposed into a sequence of rigid links and virtual 6-DOF springs, which includes:
(a) a rigid link between the manipulator base and the ith actuating joint (part of the base platform);
(b) a 1-DOF actuating joint allowing one translation ρ_{i0};
(c) a rigid foot;
(d) a 6-DOF virtual spring describing the foot stiffness;
(e) a 1-DOF passive R-joint at the beginning of the leg allowing one rotation with angle ρ_{i1};
(f) a rigid leg linking the foot and the end-effector;
(g) a 6-DOF virtual spring describing the leg stiffness;
(h) a 1-DOF passive R-joint at the end of the leg 2 (not for leg 1) allowing one rotation with angle ρ_{22};
(i) a rigid link from the manipulator leg to the end-effector (part of the movable platform).

From these assumptions, the matrix regrouping the stiffness matrices of all segments of the leg i has the following form [16]:

$$\mathbf{K}_{\mathrm{elt}}^i = \begin{bmatrix} \mathbf{K}_{\mathrm{Foot}}^i & \mathbf{0}_{6\times6} \\ \mathbf{0}_{6\times6} & \mathbf{K}_{\mathrm{Leg}}^i \end{bmatrix} . \qquad (46)$$

---

[2] In the paper, _P_ stands for an actuated prismatic pair and _R_ for a passive revolute joint.

For obtaining matrices $\mathbf{J}_{\mathbf{p}i}$ and $\mathbf{J}_{\mathbf{\theta}i}$ of (31), let us now consider the corresponding mathematical expression defining the end-effector location subject to variations of all the above defined coordinates of a single kinematic chain i may be written as follows:

$$\mathbf{T}^1 = \mathbf{T}^1_{Base}\mathbf{V}_a(\rho_{10})\mathbf{T}^1_{Foot}\mathbf{V}_s(\theta_{11_1},...,\theta_{11_6})\mathbf{V}_{r1}(\rho_{11})\mathbf{T}^1_{Leg}$$
$$\cdot \mathbf{V}_s(\theta_{12_1},...,\theta_{12_6})\mathbf{T}^1_{Tool} \quad (47)$$

$$\mathbf{T}^2 = \mathbf{T}^2_{Base}\mathbf{V}_a(\rho_{20})\mathbf{T}^2_{Foot}\mathbf{V}_s(\theta_{21_1},...,\theta_{21_6})\mathbf{V}_{r1}(\rho_{21})\mathbf{T}^2_{Leg}$$
$$\cdot \mathbf{V}_s(\theta_{22_1},...,\theta_{22_6})\mathbf{V}_{r2}(\rho_{22})\mathbf{T}^2_{Tool} \quad (48)$$

where the matrix function $\mathbf{V}_a(\cdot)$ is an elementary translation along $\mathbf{y}$, the matrix functions $\mathbf{V}_{rj}(\cdot)$ ($j = 1, 2$) are elementary rotations around $\mathbf{z}$, the spring matrix $\mathbf{V}_s(\cdot)$ is composed of six elementary transformations defined by the coordinates $(\theta_{ij_1},...,\theta_{ij_6})$ of the virtual joints $(i, j = 1, 2)$. Matrices $\mathbf{T}^i_{Base}$, $\mathbf{T}^i_{Foot}$ and $\mathbf{T}^i_{Leg}$ represents the rigid displacements of the base, foot and leg, respectively [16] (Fig. 3).

The matrix $\mathbf{J}_{\mathbf{\theta}i}$ may be obtained from the derivation of the matrix $\mathbf{T}^i$ with respect to the spring parameters θ_{ij_v} ($v = 1$ to 6), at the point $\theta_{ij_v} = 0$, considering that

$$\frac{\partial \mathbf{T}^i}{\partial \theta_{ij_v}} = \mathbf{H}^L_{ij}\frac{\partial \mathbf{V}_s}{\partial \theta_{ij_v}}(\theta_{ij_v})\mathbf{H}^R_{ij} = \begin{bmatrix} 0 & -\varphi'_{iz} & \varphi'_{iy} & p'_{ix} \\ \varphi'_{iz} & 0 & -\varphi'_{ix} & p'_{iy} \\ -\varphi'_{iy} & \varphi'_{ix} & 0 & p'_{iz} \\ 0 & 0 & 0 & 0 \end{bmatrix}. \quad (49)$$

where the first and the third multipliers are the constant homogenous matrices which do not include the displacement θ_{ij_v}, and the second multiplier corresponds to the derivative of the elementary translation or rotation corresponding to θ_{ij_v}. In the right-hand term, symbol " ' " denotes the first derivative of the variables with respect to θ_{ij_v}. Therefore, p'_{ix}, p'_{iy} and p'_{iz} (resp. φ'_{ix}, φ'_{iy} and φ'_{iz}) correspond to the small translations along (resp. rotations about) $\mathbf{x}$, $\mathbf{y}$ and $\mathbf{z}$ axes of the extremity of the leg i due to the variation of the parameter θ_{ij_v}.

The Jacobians $\mathbf{J}_{\mathbf{p}i}$ can be computed in a similar manner, but the derivatives are evaluated in the neighborhood of the "nominal" values of the passive joint coordinates ρ_{ij} corresponding to the rigid case (these values are obtained from the inverse kinematics).

Finally, the stiffness matrix $\mathbf{K}_i$ of the leg i, which relates the deformations $\delta\mathbf{t}$ to the force $\mathbf{f}_i$ can be computed by direct inversion of relevant 7 by 7 (8 by 8 in the case of the leg 2) matrix in the left hand side of the following equation [16]

$$\begin{bmatrix} \mathbf{S}_{\mathbf{\theta}i} & \mathbf{J}_{\mathbf{p}i} \\ \mathbf{J}^T_{\mathbf{p}i} & 0 \end{bmatrix}\begin{bmatrix} \mathbf{f}_i \\ \mathbf{p}_i \end{bmatrix} = \begin{bmatrix} \delta\mathbf{t} \\ 0 \end{bmatrix}, \quad \mathbf{S}_{\mathbf{\theta}i} = \mathbf{J}_{\mathbf{\theta}i}(\mathbf{K}^i_{elt})^{-1}\mathbf{J}^T_{\mathbf{\theta}i} \quad (50)$$

and by extracting the 6 by 6 sub-matrix with indices corresponding to $\mathbf{S}_{\mathbf{\theta}i}$.

After the stiffness matrices $\mathbf{K}_i$ for all kinematic chains

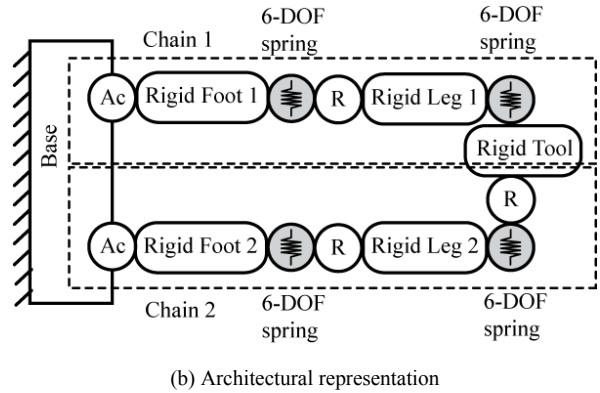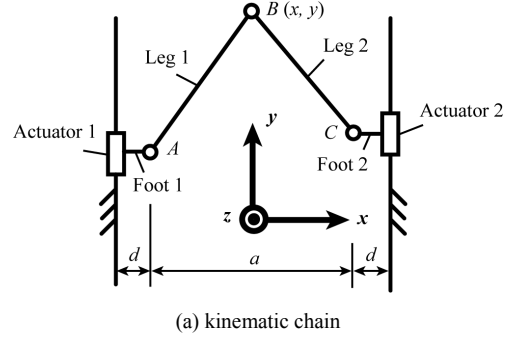

(a) kinematic chain

(b) Architectural representation

Fig. 3. Description of the *PRRRP* manipulator.

are computed, the stiffness of the entire manipulator can be found by simple addition:

$$\mathbf{K}_{\mathbf{r}} = \sum_{i=1}^{n}\mathbf{K}_i. \quad (51)$$

Using expressions (46) to (51), all relations of sections II.C and II.D can be computed. Let us now compare the results obtained by the presented procedure with a more general method.

For this simulation, each link is modelled as a beam of constant cross-section. The stiffness matrix expressions for beams are given in [16]. Then, the following numerical parameters are used:
- length of segments: $AB = AC = 0.5$ m, $a = 0.33$ m, $d = 0.1$ m;
- Young modulus: $E_{foot} = E_{Leg} = 210$ GPa; Poisson coefficients: $\nu_{foot} = \nu_{Leg} = 0.3$;
- Each beam has the same cross-section represented by a circle of radius 0.05 m;
- Material density: $\rho_{foot} = \rho_{Leg} = 7800$ kg/m^3.

Our model will be compared with one created using the FEA software Castem [19]. In the FEA model, all links are modelled using 3D beam finite elements (10 elements by beam). As for one fixed position along $\mathbf{x}$ axis of the robot, the configuration is invariant for any position along $\mathbf{y}$ axis, only the position along $\mathbf{x}$ axis will vary. The results are presented in Table 1.

In this table, it is shown that, for our model, the value of the first natural frequency is obtained with at most 4% error. This is almost sufficient for using such algorithm in

Position along x axis	First natural frequency (Hz)			Second natural frequency (Hz)			Third natural frequency (Hz)		
	FEA	Our model	% error	FEA	Our model	% error	FEA	Our model	% error
$x = 0$ m	204.65	210.48	2.85	555.51	556.58	0.19	787.09	903.57	14.80
$x = 0.05$ m	204.85	210.71	2.86	558.10	558.64	0.10	786.97	906.63	15.21
$x = 0.1$ m	205.46	211.44	2.91	565.98	566.85	0.15	786.60	910.46	15.75
$x = 0.15$ m	206.53	212.75	3.01	579.52	581.39	0.32	785.98	916.76	16.64
$x = 0.2$ m	208.19	214.80	3.17	599.36	602.32	0.49	785.12	929.35	18.37
$x = 0.25$ m	210.75	218.02	3.45	626.64	628.86	0.35	784.06	956.93	22.05
$x = 0.3$ m	215.25	223.88	4.01	664.27	658.27	0.90	782.99	1023.64	30.73

TABLE 1. Values of the three first natural frequencies of the *PRRRP* robot under study computed with two different methods: (i) using a FEA model and (ii) using the proposed method.

design procedure. Moreover, this percentage decreases to 0.9% for the second natural frequency. However, the value of the third frequency has quite a large percentage of uncertainty. Indeed, this is due to the fact that the displacements due to the two first frequencies are very close from the displacement of the robot when a load is applied at the end effector, which is not the case for the third frequency.

These results confirm the validity of our hypotheses and of our approach. It should be also mentioned that the Castem software computes the results in 0.09s while our approach takes 0.006 s, i.e. our procedure runs 15 times faster (for a Pentium 2.53 GHz, 4 Gb of RAM). Even if both computation times are very small in this example, in design optimization loops, for which thousands of possible configurations are tested, this saving of time is of the utmost importance.

IV. Conclusions

This paper has presented an approach for computing the first natural frequencies of parallel robots. The approach, based on the Rayleigh-Ritz approximation, aims at reducing the model dimension by decreasing the size of the matrices describing the robot mass and stiffness. This saves computational time, avoiding inaccuracy due to ill-conditioning and thus can be used in design procedure as well as in real-time control. Simulations have been carried out on a *PRRRP* robot modelled in 3D and comparisons have been achieved with FEA software. The obtained results confirm the validity of the proposed procedure and shows that the algorithm runs 15 times faster than a classical FEA method.

Acknowledgements

References

[1] Brogardh, T. Present and future robot control development – an industrial perspective, Annual Reviews in Control, 31 (1):69–79, 2007.
[2] Chanal, H., Duc, E. and Ray, P. A study of the impact of machine tool structure on machining processes. International Journal of Machine Tools and Manufacture, 46 (2):98–106,2006.
[3] Singer, N. Residual vibration reduction in computer controlled machines," PhD thesis, Department of Mechanical Engineering, MIT, Fall, 1988.
[4] Singhose, W., Singer, N., and Seering, W. Comparison of command methods for reducing residual vibrations. Proceedings of the 1995 European Control Conference, Rome, Italy 5-8 September, 1995.
[5] Pelaez, G., Pelaez, Gu., Perez, J.M., Vizan, A., Bautista, E. Input shaping reference commands for trajectory following Cartesian machines. Control Engineering Practice, 13:941-958, 2005.
[6] Voglewede, P.A. and Ebert-Uphoff, I. Overatching framework for measuring the closeness to singularities of parallel manipulators. IEEE Transactions on Robotics, 21(6):1037–1045, 2005.
[7] Bouzgarrou, B.C., Fauroux, J.C., Gogu, G. and Heerah, Y. Rigidity analysis of T3R1 parallel robot uncoupled kinematics. Proceedings of the 35th International Symposium on Robotics, Paris, March, 2004.
[8] Briot, S., Pashkevich, A. and Chablat, D. On the optimal design of parallel robots taking into account their deformations and natural frequencies. ASME 2009 IDETC/CIE, San Diego, California, USA, August, 2009.
[9] Shabana, A.A. Dynamics of multibody systems. 3rd Ed. Cambridge University press.
[10] Cammarata, A. and Sinatra, R. The elastodynamics of a 3-CRU spherical robot. Proc. of the 2nd Int. Workshop on Fund. Issues an Future Rob. Res. Dir. for Parallel Mech. and Manip., Montpellier, France, September 21–22, 2008.
[11] Bettaieb, F., Cosson, P. and Hascoët, J.-Y. Modeling of a high-speed machining center with a multibody approach: the dynamic modeling of flexible manipulators. Proceedings of the 6th International Conference on High Speed Machining, San Sebastian, Spain, March 21-22, 2007.
[12] El-Khasawneh, B.S. and Ferreira, P.M. Computation of stiffness and stiffness bounds for parallel link manipulators, International Journal of Machine Tools and Manufacture, 39(2):321-342,1999.
[13] Deblaise, D., Hernot, X. and Maurine, P. Systematic analytical method for PKM stiffness matrix calculation. Proceedings of the IEEE ICRA, Orlando, Florida, May, pages 4213–4219, 2006.
[14] Imbert, J. F. Analyse des structures par éléments finis. Cepadues Editions, 1979.
[15] Wittbrodt, E., Adamiec-Wojcik, I. and Wojciech, S. Dynamics of flexible multibody systems. Springer-Verlag, 2006.
[16] Pashkevich A., Chablat D. and Wenger P. Stiffness analysis of overconstrained parallel manipulators. Mechanism and Machine Theory, 44(5):966–982, 2009.
[17] Birkhoff, G., De Boor, C., Swartz, B., and Wendroff, B. Rayleigh-Ritz approximation by piecewise cubic polynomials, SIAM Journal on Numerical Analysis, 3(2):188-203, 1966.
[18] Blevins, R.D. Formulas for natural frequency and mode shape. Krieger Publishing Company, Malabar, Florida, 1979.
[19] http://www-cast3m.cea.fr/cast3m/index.jsp.